Distributed Feedback Laser Biosensor Noise Reduction

Yafang Tan, Allen Chu, Meng Lu, and Brian T. Cunningham, *Fellow, IEEE*

***Abstract*— Label-free biosensors based upon detection of shifts in the emission wavelength, which occur when biological analytes are adsorbed on the surface of a solid-state laser, represent an important new class of sensors that can simultaneously provide high sensitivity and high resolution. We report on a signal processing approach that enables detection of lasing wavelength shifts as small as $\Delta\lambda \sim 1.5$ pm from a distributed feedback laser biosensor (DFBLB) fabricated upon a flexible plastic substrate and incorporated into standard-format microplates. Because the DFBLB can be optically pumped in a pulsed mode at a repetition rate that is substantially faster than the rate of biomolecular binding interactions, noise may be reduced through the ability to average multiple independent readings through integration of many lasing spectra within a single spectral integration period, and to subsequently use boxcar averaging to collapse multiple readings in a time sequence to a single time point. We have observe that the DFBLB occasionally produces nonclassical output spectra that can lead to an increase in wavelength shift noise, and therefore we implement a statistical metric to automatically determine whether an acquired spectrum should be discarded from analysis. The combined approaches are used to demonstrate the ability to detect a protein–protein interaction with an analyte concentration that would not otherwise be observable over background noise.**

***Index Terms*— Distributed feedback, label-free, laser biosensor, noise reduction.**

I. Introduction

In order for label-free biosensors to have an impact on the most challenging detection applications, they must simultaneously provide high sensitivity, large dynamic range, and resolution sufficient for detection of mass density changes less than < 1 pg/mm^2, with values in this range for several optical biosensors compared in a recent review [1]. Resonant optical biosensors represent a class of devices that have been widely adopted in applications that include pharmaceutical high throughput screening, environmental monitoring, life science research, and diagnostic testing. Until recently, resonant optical biosensors were mainly comprised of passive optical structures such as gold films for surface plasmon resonance (SPR) [2]–[5], photonic crystals [6]–[10], circular whispering gallery mode resonators [11]–[18] that interact with an external light source via reflection, transmission, or waveguide coupling. In order to achieve improved resolution, these approaches seek to provide passive resonators with greater resonant quality factor, defined as $Q \equiv \lambda_0/\Delta\lambda_0$, where λ_0 represents the resonant wavelength, and $\Delta\lambda_0$ represents the spectral width of the resonance at one-half of the peak intensity. In general, a tradeoff is obtained in which greater Q also results in reduced sensitivity as measured by the wavelength shift obtained for an adsorbed biomolecular mass density. A high Q resonator may also efficiently constrain its resonant electric field largely within the dielectric material of the sensor structure, so that the electric field that has the opportunity to interact with adsorbed biomolecules may only extend a few nanometers into the surrounding liquid medium. In this case, the dynamic range of a sensor may not be sufficient for detection experiments involving surface chemistry layers, large capture molecules such as antibodies, and high molecular weight analytes.

The distributed feedback laser biosensor (DFBLB) represents a departure from passive optical resonator biosensors because the structure incorporates its own source of optical gain and feedback, so that it can achieve narrow bandwidth output through the process of stimulated emission. As shown in previous publications, the DFBLB can be fabricated upon glass [19] or flexible plastic substrates [20], [21] by nanoreplica molding so that the sensor can be incorporated into the bottom surfaces of all the wells in a standard format 384-well microplate [22]. As shown in Fig. 1, the DFBLB device structure is comprised of a low refractive index polymer thick film ($n = 1.39$, $t \sim 100\ \mu$m) that is molded with a linear grating upper surface structure (period $\Lambda = 400$ nm, grating depth $d = 40$ nm). The grating is coated with a higher refractive index layer dye-doped SU-8 ($n = 1.58$, $t = 300$ nm) which provides horizontal confinement of the lasing mode and a source of gain. When applied using a horizontal dipping process, the SU-8 layer planarizes the surface relief of the underlying grating [23]. In order to improve detection sensitivity by biasing lasing modes towards the liquid media that covers the DFBLB surface, a thin film of TiO_2 ($n = 2.1$, $t = 10$ nm) is applied over the SU-8 layer. Full details of the

Manuscript received April 2, 2012; revised October 24, 2012 and January 6, 2013; accepted January 20, 2013. Date of publication February 4, 2013; date of current version April 10, 2013. This work was supported in part by the National Institutes of Health under Grant R21-EB009695-A, the National Science Foundation under Grant ECCS-09-24062, and the Telemedicine and Advanced Technology Research Center, under Contract W81XWH0810701. The associate editor coordinating the review of this paper and approving it for publication was Dr. Alexander Fish.

Y. Tan, A. Chu, and M. Lu are with the Department of Electrical and Computer Engineering, University of Illinois at Urbana-Champaign, Urbana, IL 61801 USA (e-mail: tan50@illinois.edu; chu32@illinois.edu; menglv@gmail.com).

B. T. Cunningham is with the Department of Electrical and Computer Engineering and the Department of Bioengineering, University of Illinois at Urbana-Champaign, Urbana, IL 61801 USA (e-mail: bcunning@illinois.edu).

Color versions of one or more of the figures in this paper are available online at http://ieeexplore.ieee.org.

Digital Object Identifier 10.1109/JSEN.2013.2244591

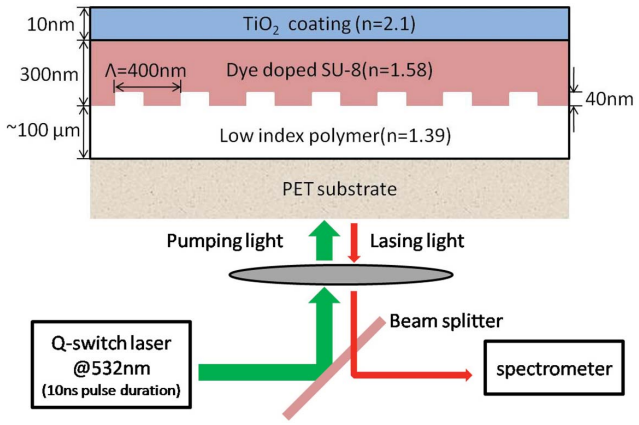

Fig. 1. Schematic cross-sectional diagram of the DFBLB structure and detection instrument. The dye-doped SU8 layer provides both light confinement along the horizontal direction and amplification of the oscillation mode, while the TiO_2 top layer contributes to spatial mode bias into the liquid medium. The device is pumped by a pulsed Q-switched laser and the signal is detected by a spectrometer.

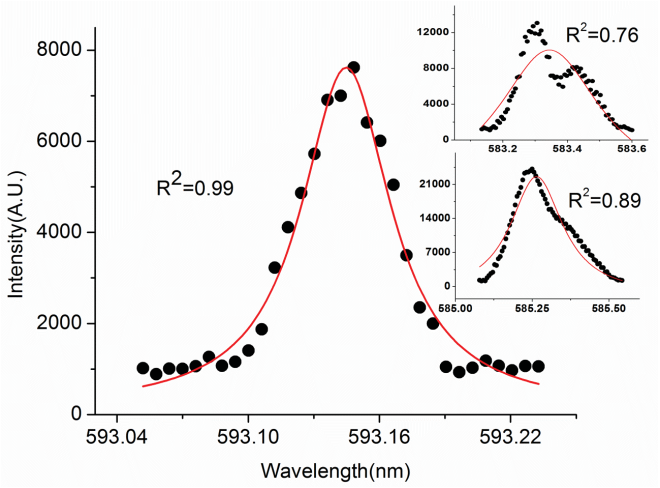

Fig. 2. Fitted spectra of DFBLB output displaying either single mode or double mode operation. The black dots represent points gathered by the spectrometer, and the red curves are Lorentzian functions that best fit the measured spectra. The R^2 parameter (defined in the text) quantifies the degree of fit between the Lorentzian function and the measured spectrum.

fabrication process are provided in [23]. Operation of the DFBLB detection instrument is also summarized in Fig. 1. The DFB cavity is based on a second order Bragg grating that supports a vertically emitting mode by first-order diffraction. The device is optically excited by a frequency doubled, Q-switched Nd: YAG laser ($\lambda = 532$ nm, 10 ns pulse width, single pulse mode) through a 200 μm diameter fiber and a focusing lens beneath the sensor surface. The emission from the DFB laser biosensor is coupled to a spectrometer (Horiba 550) through a detection fiber bundled with the excitation fiber. As shown in previous work [24], the dependence of the relative laser pulse energy on the pump fluence exhibits a clear threshold fluence of $\sim$1.0 μJ-mm^{-2}. The laser emission spectrum generally fits a Lorentzian profile, which is fit mathematically to determine the center wavelength. The lasing output has a spectral linewidth of $\Delta\lambda = 0.05$ nm at an emission wavelength of $\lambda \sim 590$ nm, resulting in a quality factor of $Q = 10^4$. The sensitivity and dynamic range of the DFBLB have been demonstrated to share similarities to its passive counterpart, the photonic crystal biosensor [25]. The DFBLB demonstrates single mode operation over a total wavelength range of 20 nm in which the lasing wavelength is linearly proportional to the bulk refractive index of the liquid media on its surface [22]. A bulk refractive index sensitivity, as defined by $S_b = \Delta\lambda/\Delta n$, (where $\Delta\lambda$ is the shift in lasing wavelength when the sensor surface is exposed to a bulk refractive index change of Δn) of $S_b = 100$ nm/RIU (RIU = refractive index units) has been obtained for previous devices, which is not as large as that obtained for SPR ($S_b = 1000$ nm/RIU, $Q = 10$ [1]) and photonic crystal biosensors ($S_b = 300$ nm/RIU, $Q = 1000$ [26]), but larger values reported for microring resonators ($S_b = 36$ nm/RIU, $Q = 1000$ [27]) and microtoroids ($S_b = 30$ nm/RIU, $Q = 106$ [28]) .

In order to fully take advantage of the potential gains in resolution from a sensor with high Q, it is necessary to measure the resonant wavelength with as small of a standard deviation as possible. Because the DFBLB is operated in a pulsed mode, in which we wish to accurately determine the wavelength of laser emission directed vertically from the device surface, determination of wavelength shifts must be considered slightly differently than how one typically measures resonant wavelength from a passive resonator. First, the pump source provides short 10 ns pulses, resulting in a measurement that samples the biosensor surface for a very precisely defined time. However, the duty cycle of pumping is extremely low (10^{-7}) because the rate of pump pulses is 1-10 Hz, resulting in an overall pump energy density of only 10 μW. As a result, we have not observed gradual heating of the sensor when conducting continuous measurements over extended periods of time. Each pump pulse results in the delivery of laser emission photons to a discrete set of sensor pixels within the spectrometer, in order to produce a spectrum. If multiple pump pulses are provided to the sensor within the integration time of the spectrometer, then the spectrum effectively accumulates several discrete lasing pulse outputs, representing a form of averaging. Ideally, the accumulated spectrum resembles the plot shown in Fig. 2, in which the discretized pixels of the spectrometer combine to form a smooth single mode spectrum that can be fit accurately with a mathematical function such as a Lorentzian. However, a potential noise source for measuring the output of DFBLBs results from lack of pump intensity repeatability from one pulse to the next. For example, the intensity of pump pulses may vary by as much as 150% from pulse to pulse, resulting in output pulses that also have highly variable intensities. Deviation in laser emission intensity can subsequently have a substantial effect on the accumulated lasing spectrum measured on the spectrometer. Therefore, it is important to determine whether a lasing spectrum should be obtained from a single pulse, many pulses, or some intermediate value–as a means to achieving the lowest noise in lasing wavelength measurements.

We have also observed the random occurrence of emission spectra that do not fit our desired single mode characteristic.

For example, the lasing output will sometimes contain two apparent modes as shown in the inset of Fig. 2, where the second mode may either be close or far from the main mode. In some instances, such behavior occurs either once, or for a small number of measurements, after which the sensor returns to single mode operation. In other cases, a device will begin to display multimode behavior and remain in that state. Such multiple mode phenomena were observed in 20 percent of the sensors in a 384-well microplate and have not reported previously by other research groups studying plastic-based laser biosensors [29].While we have worked to identify the cause of this issue and to remedy it through elimination of surface defects or other physical damage, its occurrence has a substantial negative effect on the ability of the peak fitting algorithm to accurately determine the lasing wavelength, as shown by the poor fit of Lorentzian curves to the measured spectra in Fig. 2 (inset). As a result, we have also incorporated a mechanism by which the detection instrument software can automatically determine whether or not the lasing emission spectra is well-behaved or not, and to remove from analysis any peaks that do not fit the desired profile.

Finally, for many biomolecule interaction measurements, one wishes to measure the wavelength shift induced from a baseline state (before an analyte is bound) which occurs before an analyte is exposed to the sensor, to a post-binding equilibrium state which occurs after the analyte has had opportunity to bind with its capture molecule and reach a new steady state. In this case, detection of the wavelength shift between two states can be achieved with lower noise through the averaging of independent measurements in each of the two states. Noise is quantitatively characterized as the standard deviation,

$$\sigma = \sqrt{\frac{1}{M}\Sigma_{i=1}^{M}(x_i - \mu)^2} \tag{1}$$

where x_i is the measured data, M is the total number of measurements and μ is the mean value of the multiple measurements. A laser wavelength shift of three standard deviations above background noise has a 99.7% likelihood of being a measurable signal. Thus, the measurable wavelength shift therefore should be larger than 3σ to be considered statistically distinct from background noise [30]. The commonly used "boxcar" technique, in which the reported measurement for a particular point in time is the average of measurements taken both before and after that time, can reduce noise by $\sqrt{N}$, where N is the number of averaged independent measurements of the DFBLB emission wavelength.

In this work, we study the effects of these three approaches on the low-noise measurement of lasing wavelength from a plastic-based DFBLB in microplate format. We first apply a fitting coefficient to automatically exclude emission spectra that deviate from a Lorentzion model. We examine the influence of the external pump repetition rate to determine the extent to which multi-pulse accumulation in the measured spectrum effects the ability to measure the lasing wavelength accurately, finding that increasing the repetition rate results in lower noise. We also compared the noise calculated from temporally averaged measurements within one well to show that boxcar averaging further reduces the laser wavelength noise as expected. Using all three approaches together, we are able to reliably measure wavelength shifts as small as 1.5 pm, as determined by 3σ ($\sigma = 0.5$ pm). Dose-response characterization is performed for a protein-protein interaction, in which immobilized Protein A is used to capture an antibody from a test sample.

II. Methods and Results

A. Determining Presence of Single Mode Operation and Rejection of Nonclassical Spectra

Optical pumping of the DFBLB generally results in single mode lasing output, with a spectral characteristic measured by the spectrometer that can be fit to a Lorentzian function. The lasing wavelength value (LWV) for a biosensor measurement is defined as the wavelength of peak output intensity. Because the measured spectrum is comprised of discrete points separated by wavelength steps of $\Delta\lambda = 0.0265$ nm, LWV can be estimated with better resolution that the wavelength resolution of the spectrometer by mathematically determining the peak wavelength of the Lorentzian function that fits the measured points. This method is valid as long as the Lorentzian function fits the measured spectrum closely. However, deviations of the actual lasing spectrum from the Lorentzian curve are often observed as shown in the inset of Fig. 2, where more than one lasing mode is present. The curve-fitting algorithm, unable to match the data to the expected Lorentzian function, reports a LWV that is no longer representative of the actual lasing wavelength. In fact, because two modes are present, the lasing wavelength is poorly defined, and LWV noise in the range of 50–100 pm is introduced as the magnitudes of the two modes change with respect to each other.

Therefore, it is necessary to introduce a quantity to describe how well the measured spectrum represents a classical Lorentzian profile, and a threshold for rejecting spectra that will result in elevated LWV noise. Here, we use the coefficient of determination (R^2) as defined by $R^2 \equiv 1 - SS_{err} / SS_{tot}$, where SS_{err} is the sum of squares of residuals and SS_{tot} is the total sum of squares. R^2 is a commonly used statistic that describes how well actual outcomes are likely to be predicted by a model [31]. The value of R^2 will be $0 < R^2 < 1$, where $R^2 = 1$ represents a perfect fit of the data to the model. Fig. 2 demonstrates the calculation of R^2 for several representative spectra. We observe that when $R^2 < 0.8$, the measured data deviates so much from the fitted curve that the LWV values are no longer meaningful. Therefore, we have selected a threshold value of $R^2 > 0.8$ for a sensor spectrum to be considered acceptable for further analysis. If a sensor begins to demonstrate multimode output behavior, the algorithm automatically identifies it, and flags the sensor so its output may be disregarded. A sensor that transiently demonstrates multimode output may also be identified, and elevated LWV noise from this mechanism may be eliminated.

B. Determination of Optimal Pump Repetition Rate

To study the effect of pump repetition rate, the integration time for the spectrometer was set to 500 ms and pumping rates

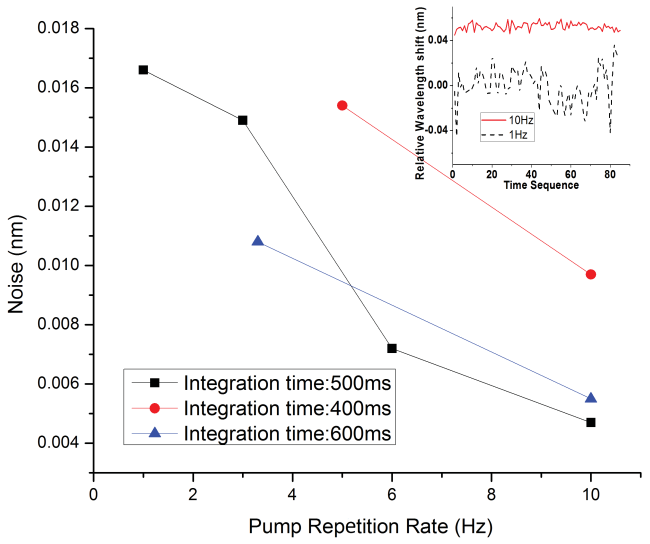

Fig. 3. Standard deviation (σ) calculated from a sequence of independent measurements plotted as a function of the external pumping repetition rate. Increasing the camera integration time (400, 500 and 600 ms) results in accumulation of an increasing number of DFBLB pulses into a single spectrum. Accumulation of multiple pulses is observed to decrease the standard deviation for DFBLB output wavelength through both increased pump repetition rate and increased integration time.

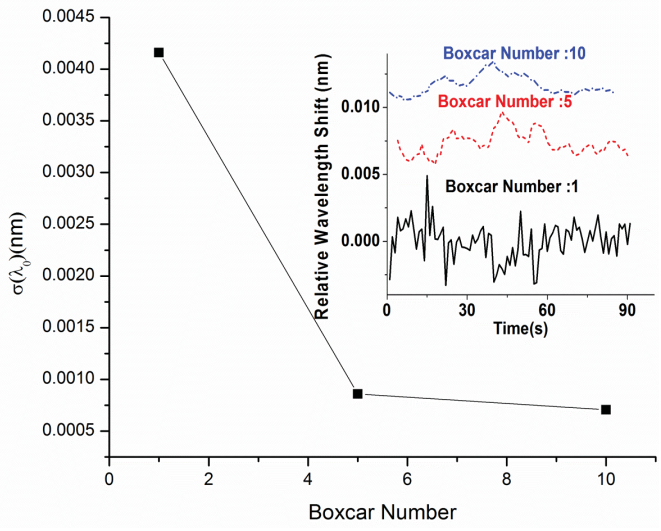

Fig. 4. Standard deviation (σ) calculated from multiple measurements for a time sequence that represents the noise amplitude is plotted as a function of the boxcar number. The noise decreased from 4 to 0.5 pm as the number of independent measurements combined into a single output is increased from 1 to 10. The inset of Fig. 4 illustrates the dynamic variation of the averaged lasing wavelength over a 90 s period.

of 1 Hz, 3 Hz, 6 Hz, and 10 Hz were compared. The highest pump rate of the Nd:Yag laser used in this work is 10 Hz due to the thermal loading effect of its flash lamp. A DFBLB was prepared in microplate format, and covered with water media, with no other variable. For each pump rate, the standard deviation (σ) was calculated from 85 discrete measurements. The inset of Fig. 3 compares the dynamic LWV readout over time sequences with pump rates of 1 Hz and 10 Hz. We observe that the noise amplitude decreases with increasing pump rate, as a single gathered spectrum is comprised of the combined output of a greater number of pulse outputs within a fixed duration, resulting in a more pronounced "peak" in the measured spectrum. This effect is further confirmed through changing the integration time of the spectrometer (400 ms and 600 ms), as shown in Fig. 3. A further observation is that the noise decreases as the integration time is increased for a fixed pump rate, which indicates that the gathered spectrum can be fit more accurately as the more outputs are accumulated. Beyond an integration time of 600 ms and pump rate of 10 Hz pumping, the noise is not reduced further.

C. Temporal Averaging

Time averaging is a common way to reduce random noise by canceling out random errors. Provided that independent measurements are gathered at a rate that is much faster than the rate of the biomolecular binding process that is being measured, boxcar averaging will have only a minor effect on measurements on the rate of a biomolecular interaction, and no effect if one is interested only in the endpoint of a measurement. To further reduce noise, a boxcar method was studied. It is the simplest form of smoothing which replaces each data value with the average of neighboring values. In equation form, the moving average is calculated by:

$$\bar{x}[i] = \frac{1}{N}\Sigma_{j=1}^{N} x[i+j], \tag{2}$$

where N is the number of the averaging values. The boxcar method can reduce noise by $\sqrt{N}$, where the noise is characterized by the standard deviation σ calculated from the multiple independent measurements [32]. A single spot in a DFBLB biosensor microplate well was pumped 90 times with 0.5s intervals between LWV determinations. Boxcar averaging was applied to the data using $1 \leq N \leq 10$. The integration time of the CCD was set to 500 ms and the external pump rate was 10 Hz. The black curve in Fig. 4 shows that the noise decreased from $\sigma = 4$ pm to $\sigma = 0.5$ pm as the boxcar number N increased from 1 to 10. The inset of Fig. 4 illustrates the dynamic variation of the averaged lasing wavelengths. We observe that determination of the lasing wavelength is improved by temporal averaging. However, such improvement results in a dramatic decrease in the scanning speed required for gathering kinetic data, as a boxcar length of $N = 10$ corresponds to 50 pulses gathered over a time span of 5 seconds. For instances in which we are concerned only with the laser wavelength shift of the sensor between two stable states, such as before and after exposure of the sensor to an analyte, averaging of several independent wavelength measurements in each of the two states can be carried out without concern for the effect of temporal averaging on the kinetic sensor response. This approach was applied to the dose-response characterization of the interaction between an immobilized protein and an analyte protein in solution.

Protein A was attached to the DFBLB surface using covalent bonds by functionalizing the sensor surface aldehyde-based surface chemistry. To functionalize the sensor surface, each well was treated with a 10% solution of polyvinylamine (PVA;

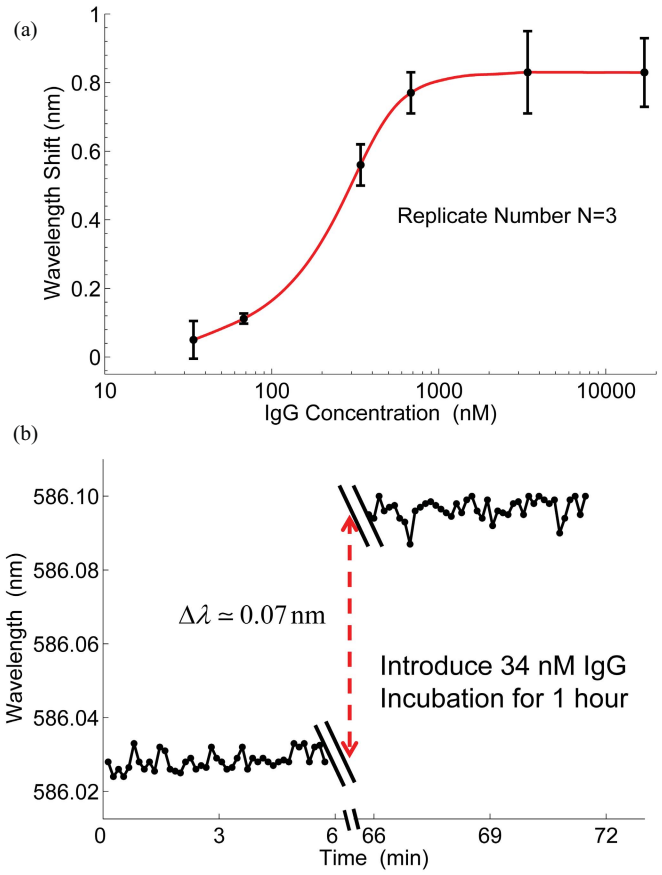

Fig. 5. (a) Laser wavelength shift end point as a function of rabbit IgG concentration for DFBLB sensors prepared with capture Protein A. The error bars represent the standard deviation from three replicate experiments from separate sensors. (b) Detection kinetics for human IgG at 34 nM with spectra measured every 8 s.

provided by SRU Biosystems Inc.) in water and incubated at 40 °C for 2 hours. All wells were then washed 3 times with water. Each well of the sensor was then exposed to 50 μL glutaraldehyde solution (25% in water; Sigma–Aldrich) for 4 hours, followed by a wash step. Next, a measurement of the emission wavelength from the PBS-immersed laser surface was made and recorded. Protein A (Sigma-Aldrich; MW = 40 kDa) was dissolved in 0.01M phosphate buffered saline (PBS; pH = 7.4) solution to a concentration of 0.5 mg/ml, pipetted into the active wells with 20 μL volume, and allowed to incubate for 20 min at room temperature. The emission wavelengths were taken again and the shift from Protein A adsorption was $\Delta\lambda = 0.67 \pm 0.05$ nm.

After Protein A was immobilized on the sensor, it was exposed to a rabbit antibody under a range of concentrations. All of the wells in the sensor microplate were first rinsed and soaked in PBS buffer to establish an initial baseline LWV. Three wells were used as reference wells, while eighteen were active wells. Prior to introduction of the IgG solution, the wells were rinsed 3x with PBS, filled with 20 μL PBS, and the lasing wavelengths were recorded for a ~11min duration. Rabbit IgG (Sigma-Aldrich, Mw = 146 kDa) was dissolved in 0.01M PBS solution in six different concentrations (17, 3.4, 0.68, 0.34 μM and 68, 34 nM). The PBS solution in the active wells was then replaced with 20 μL of rabbit IgG solution. Three replicate wells were used for each IgG concentration. Next, the sensor surface was allowed to stabilize for 10 min and was subsequently rinsed with PBS solution to remove any unbound IgG. Fig. 5 (a) shows the laser wavelength shift end point as a function of rabbit IgG concentration. The error bars represent one standard deviation calculated from the three replicates. As an example, the LWV data taken before and after the IgG exposure are shown for an IgG concentration of 34 nM in Fig. 5 (b) with spectra measured every 8 s. The detected signal for the high concentration (17 μM rabbit IgG) approaches saturation due to the limited number of protein A binding sites on the sensor surface. The lowest concentration of rabbit IgG (34 nM) resulted in an easily measured laser wavelength shift of $\Delta\lambda = 70$ pm, which demonstrates detection sensitivity comparable with other optical biosensor approaches [33]. Using nonlinear curve fitting to determine the inflection point of the dose-response curve, we measured a dissociation constant of $K_d = 0.53$ μM for the protein A-IgG interaction, which corresponds well with reported values [34].

III. Conclusion

In this work, we have demonstrated how a combination of detection instrument configuration and data analysis can be used to obtain low noise from DFBLB sensor measurements. We show that noise is reduced through accumulation of multiple discrete pulses from the sensor into a smooth spectrum with a Lorentzian profile, and that spurious instances of multi-mode lasing behavior, which would ordinarily increase noise substantially, can be accommodated by a statistical curve-fitting metric that automatically identifies multi-mode operation. As expected, temporal averaging of several independent sensor measurements will also reduce noise, at the expense of smoothing of kinetic sensor data. In the case in which we are only interested in wavelength shift endpoints between two states, many measurements can be averaged to obtain a large reduction in noise. Detection of wavelength shifts as small as 1.5 pm is demonstrated, which satisfies the requirement for characterization of protein-protein interactions, as demonstrated using the Protein A-IgG system. The dynamic binding curve shows no spurious data with the use of the signal processing methods including R^2 filtering, temporal averaging and pump repetition rate optimization. The small wavelength shift of 0.07 nm would not otherwise be detectable over the background noise.

Acknowledgment

The authors would like to thank the support staff of Micro and Nanotechnology Laboratory at the University of Illinois at Urbana-Champaign.

References

[1] X. Fan, I. M. White, S. I. Shopova, H. Zhu, J. D. Suter, and Y. Sun, "Sensitive optical biosensors for unlabeled targets: A review," *Analytica Chimica Acta*, vol. 620, no. 1–2, pp. 8–26, 2008.

[2] S. Scarano, M. Mascini, A. P. Turner, and M. Minunni, "Surface plasmon resonance imaging for affinity-based biosensors," *Biosensors Bioelectron.*, vol. 25, no. 5, pp. 957–966, 2010.

[3] T. Endo, S. Yamamura, K. Kerman, and E. Tamiya, "Label-free cell-based assay using localized surface plasmon resonance biosensor," *Analytica Chimica Acta*, vol. 614, no. 2, pp. 182–189, 2008.
[4] A. A. Yanik, A. E. Cetin, M. Huang, A. Artar, S. H. Mousavi, A. Khanikaev, J. H. Connor, G. Shvets, and H. Altug, "Seeing protein monolayers with naked eye through plasmonic Fano resonances," *Proc. Nat. Acad. Sci.*, vol. 108, no. 29, pp. 11784–11789, Jul. 2011.
[5] W. P. Hall, J. Modica, J. Anker, Y. Lin, M. Mrksich, and R. P. Van Duyne, "A conformation-and ion-sensitive plasmonic biosensor," *Nano Lett.*, vol. 11, no. 3, pp. 1098–1105, 2011.
[6] S. George, I. D. Block, S. I. Jones, P. C. Mathias, V. Chaudhery, P. Vuttipittayamongkol, H. Y. Wu, L. O. Vodkin, and B. T. Cunningham, "Label-free prehybridization DNA microarray imaging using photonic crystals for quantitative spot quality analysis," *Anal. Chem.*, vol. 82, no. 20, pp. 8551–8557, Oct. 2010.
[7] C.-S. Huang, S. George, M. Lu, V. Chaudhery, R. Tan, R. C. Zangar, and B. T. Cunningham, "Application of photonic crystal enhanced fluorescence to cancer biomarker microarrays," *Anal. Chem.*, vol. 83, no. 4, pp. 1425–1430, Feb. 2011.
[8] P. C. Mathias, N. Ganesh, and B. T. Cunningham, "Application of photonic crystal enhanced fluorescence to a cytokine immunoassay," *Anal. Chem.*, vol. 80, no. 23, pp. 9013–9020, Dec. 2008.
[9] J. T. Robinson, L. Chen, and M. Lipson, "On-chip gas detection in silicon optical microcavities," *Opt. Exp.*, vol. 16, no. 6, pp. 4296–4301, 2008.
[10] B. Schmidt, V. Almeida, C. Manolatou, S. Preble, and M. Lipson, "Nanocavity in a silicon waveguide for ultrasensitive nanoparticle detection," *Appl. Phys. Lett.*, vol. 85, no. 21, pp. 4854–4856, 2004.
[11] A. M. Armani, R. P. Kulkarni, S. E. Fraser, R. C. Flagan, and K. J. Vahala, "Label-free, single-molecule detection with optical microcavities," *Science*, vol. 317, no. 5839, pp. 783–787, Jul. 2007.
[12] M. S. Luchansky and R. C. Bailey, "Silicon photonic microring resonators for quantitative cytokine detection and t-cell secretion analysis," *Anal. Chem.*, vol. 82, no. 5, pp. 1975–1981, 2010.
[13] A. J. Qavi and R. C. Bailey, "Multiplexed detection and label-free quantitation of micrornas using arrays of silicon photonic microring resonators," *Angewandte Chemie Int. Ed.*, vol. 49, no. 27, pp. 4608–4611, 2010.
[14] F. Vollmer and S. Arnold, "Whispering-gallery-mode biosensing: Label-free detection down to single molecules," *Nature Methods*, vol. 5, no. 7, pp. 591–596, 2008.
[15] F. Vollmer, S. Arnold, and D. Keng, "Single virus detection from the reactive shift of a whispering-gallery mode," *Proc. Nat. Acad. Sci.*, vol. 105, no. 52, pp. 20701–20704, Dec. 2008.
[16] I. M. White, H. Oveys, and X. Fan, "Liquid-core optical ring-resonator sensors," *Opt. Lett.*, vol. 31, no. 9, pp. 1319–1321, 2006.
[17] I. M. White, H. Oveys, X. Fan, T. L. Smith, and J. Zhang, "Integrated multiplexed biosensors based on liquid core optical ring resonators and anti-resonant reflecting optical waveguide," *Appl. Phys. Lett.*, vol. 89, no. 19, pp. 191106-1–191106-3, 2006.
[18] H. Zhu, I. M. White, J. D. Suter, P. S. Dale, and X. Fan, "Analysis of biomolecule detection with optofluidic ring resonator sensors," *Opt. Exp.*, vol. 15, no. 15, pp. 9129–9146, 2007.
[19] M. Lu, S. S. Choi, C. J. Wagner, J. G. Eden, and B. T. Cunningham, "Label free biosensor incorporating a replica-molded, vertically emitting distributed feedback laser," *Appl. Phys. Lett.*, vol. 92, no. 26, pp. 261502-1–261502-3, 2008.
[20] M. Lu, S. S. Choi, U. Irfan, and B. T. Cunningham, "Plastic distributed feedback laser biosensor," *Appl. Phys. Lett.*, vol. 93, no. 11, pp. 111113-1–111113-3, 2008.
[21] C. Ge, M. Lu, X. Jian, Y. Tan, and B. T. Cunningham, "Large-area organic distributed feedback laser fabricated by nanoreplica molding and horizontal dipping," *Opt. Exp.*, vol. 18, no. 12, pp. 12980–12991, 2010.
[22] Y. Tan, C. Ge, A. Chu, M. Lu, W. Goldshlag, C. S. Huang, A. Pokhriyal, S. George, and B. T. Cunningham, "Plastic-based distributed feedback laser biosensors in microplate format," *IEEE Sensors J.*, vol. 12, no. 5, pp. 1174–1180, May 2012.
[23] H. N. Daghestani and B. W. Day, "Theory and applications of surface plasmon resonance, resonant mirror, resonant waveguide grating, and dual polarization interferometry biosensors," *Sensors*, vol. 10, no. 11, pp. 9630–9646, 2010.
[24] C. Ge, M. Lu, Y. Tan, and B. T. Cunningham, "Enhancement of pump efficiency of a visible wavelength organic distributed feedback laser by resonant optical pumping," *Opt. Exp.*, vol. 19, no. 6, pp. 5086–5092, 2011.
[25] N. Ganesh and B. T. Cunningham, "Photonic-crystal near-ultraviolet reflectance filters fabricated by nanoreplica molding," *Appl. Phys. Lett.*, vol. 88, no. 7, pp. 071110-1–071110-3, 2006.
[26] I. D. Block, M. Pineda, C. J. Choi, and B. T. Cunningham, "High sensitivity plastic-substrate photonic crystal biosensor," *IEEE Sensors J.*, vol. 8, no. 9, pp. 1546–1547, Sep. 2008.
[27] F. F. Lupi, D. Navarro-Urrios, J. Rubio-Garcia, J. Monserrat, C. Dominguez, P. Pellegrino, and B. Garrido, "Visible light emitting Si-Rich Si_3N_4 μ-disk resonators for sensoristic applications," *J. Lightw. Technol.*, vol. 30, no. 1, pp. 169–174, 2012.
[28] H. Zhu, J. D. Suter, and X. Fan, "Label-free optical ring resonator bio/chemical sensors optical guided-wave chemical and biosensors II," vol. 8, pp. 259–279, 2010.
[29] M. B. Christiansen, J. M. Lopacinska, M. H. Jakobsen, N. A. Mortensen, M. Dufva, and A. Kristensen, "Polymer photonic crystal dye lasers as optofluidic cell sensors," *Opt. Exp.*, vol. 17, no. 4, pp. 2722–2730, 2009.
[30] I. M. White and X. Fan, "On the performance quantification of resonant refractive index sensors," *Opt. Exp.*, vol. 16, no. 2, pp. 1020–1028, 2008.
[31] A. Colin Cameron and F. A. G. Windmeijer, "An R-squared measure of goodness of fit for some common nonlinear regression models," *J. Econometr.*, vol. 77, no. 4, pp. 329–342, Apr. 1997.
[32] G. M. Hieftje, "Signal-to-noise enhancement through instrumental techniques. II. Signal averaging, boxcar integration, and correlation techniques," *Anal. Chem.*, vol. 44, no. 7, pp. 69A–78A, Jun. 1972.
[33] Y. Zhang, H. Shibru, K. L. Cooper, and A. Wang, "Miniature fiber-optic multicavity Fabry-Perot interferometric biosensor," *Opt. Lett.*, vol. 30, no. 9, pp. 1021–1023, 2005.
[34] S. C. Kuo and D. A. Lauffenburger, "Relationship between receptor/ligand binding affinity and adhesion strength," *Biophys. J.*, vol. 65, no. 5, pp. 2191–2200, 1993.

Yafang Tan received the B.S. degree in electrical and computer engineering from Tsinghua University, Beijing, China, in 2008. She is currently pursuing the Ph.D. degree as a Graduate Research Assistant under direction of Prof. B. T. Cunningham with the University of Illinois at Urbana-Champaign, Urbana, IL, USA.

Her current research interests include design and optimization of the label-free optical biosensors and their applications in life science.

Allen Chu received the B.S. degree in electrical engineering from the University of California, Los Angeles, CA, USA, in 2009. He is currently pursuing the M.S. degree as a Graduate Research Assistant under the direction of Prof. B. T. Cunningham with the University of Illinois at Urbana-Champaign, Urbana, IL, USA.

His current research interests include the development of a distributed feedback laser based biosensor and its supporting instrumentation.

Meng Lu received the B.S. degree in electrical and computer engineering from the University of Science and Technology of China, Hefei, China, in 2002, and the M.S. and Ph.D. degrees in electrical and computer engineering from the University of Illinois at Urbana-Champaign, Urbana, IL, USA, in 2004 and 2008, respectively.

He is currently with SRU Biosystems, Woburn, MA, USA, working on optical biosensors. His research at the University of Illinois at Urbana-Champaign under the direction of Dr. B. Cunningham focused on the development of optical sensor systems.

Brian T. Cunningham (F'12) received the B.S., M.S., and Ph.D. degrees in electrical and computer engineering with the University of Illinois at Urbana-Champaign, Urbana, IL, USA. His thesis research was in the field of optoelectronics and compound semiconductor material science, where he contributed to the development of crystal growth techniques that are now widely used for manufacturing solid state lasers, and high frequency amplifiers for wireless communication.

He is a Professor with the Department of Electrical and Computer Engineering and the Department of Bioengineering, University of Illinois at Urbana-Champaign, where he has been a Faculty Member since 2004. His group focuses on the development of nanophotonic surfaces, plastic-based nanofabrication methods, and novel instrumentation approaches for biodetection with applications in pharmaceutical screening, life science research, environmental monitoring, disease diagnostics, and point-of-care patient testing. At the University of Illinois at Urbana-Champaign, he serves as the Director of the Bioengineering Graduate Program and Director of the NSF Center for Agricultural, Biomedical, and Pharmaceutical Nanotechnology (CABPN). He is a founder and the Chief Technical Officer of SRU Biosystems, Woburn, MA, a life science tools company that provides high sensitivity plastic-based optical biosensors, instrumentation, and software to the pharmaceutical, academic research, genomics, and proteomics communities. Prior to founding SRU Biosystems in June 2000, he was the Manager of Biomedical Technology at Draper Laboratory, Cambridge, MA, where he directed R&D projects aimed at utilizing defense-related technical capabilities for medical applications. In addition, he served as Group Leader for MEMS Sensors at Draper Laboratory, where he directed a group performing applied research on microfabricated inertial sensors, acoustic sensors, optical switches, microfluidics, tissue engineering, and biosensors. Concurrently, he was an Associate Director of the Center for Innovative Minimally Invasive Therapy (CIMIT), a Boston-area medical technology consortium, where he led the Advanced Technology Team on Microsensors. Before working at Draper Laboratory, he spent five years with the Raytheon Electronic Systems Division developing advanced infrared imaging array technology for defense and commercial applications.

Prof. Cunningham was recognized with the IEEE Sensors Council 2010 Technical Achievement Award for the invention, development, and commercialization of biosensors utilizing photonic crystals.